The effect of alpha particle irradiation on electrical properties and defects of ZnO thin films prepared by sol-gel spin coating

M.E.I. Ahmed[a,b,*], F. Taghizadeh[a], F.D. Auret[a], W.E. Meyer[a] and J.M. Nel[a]

[a]Department of Physics, University of Pretoria, Private Bag X20, Hatfield, 0028, South Africa

[b]Department of Scientific Laboratories - Physics, Sudan University of Science and Technology, P.O Box 407, Khartoum, Sudan

*Corresponding author. Department of Physics, University of Pretoria, Private Bag X20, Hatfield, 0028, South Africa. email: elagib.2030@gmail.com

Abstract

ZnO thin films were prepared using the sol-gel spin coating technique. The structure was investigated using X-ray diffraction (XRD). The XRD spectra exhibited typical randomly orientated structure with a slight preference for growth along the (002) plane and a crystallite size of ~ 48 nm. The Schottky barrier diodes were fabricated on the synthesized ZnO thin films. The electrical properties before and after irradiating the devices with alpha particle irradiation were characterized using current-voltage (*I-V*), capacitance-voltage (*C-V*), deep-level tran-sient spectroscopy (DLTS) and Laplace-transform deep-level transient spectroscopy (L-DLTS) techniques. Pd/ZnO/n-Si/AuSb Schottky diodes exhibited good rectifying properties. Before irradiation, the DLTS spectra re-vealed one defect E_4 with activation enthalpy 0.41 eV. After irradiation, there is a new defect E_α with the activation enthalpy 0.35 eV. Laplace-transform deep-level transient spectroscopy (L-DLTS) revealed the fine structure of the E_α to be made up of 0.53 eV and 0.36 eV defects.

Keywords: ZnO thin films; Sol-gel; Alpha particle irradiation; DLTS

1. Introduction

ZnO can be used in a wide range of applications. Due to its high resistance to radiation, direct band gap of approximately 3.4 eV and large exciton binding energy of 60 meV at room temperature, these applications include solar cell window layers, piezo-electric sensors, UV detectors and a variety of similar applications for space deployment [1]. ZnO thin films can be synthesized by different techniques such as pulsed laser deposition, chemical vapour deposition, spray pyrolysis and sol-gel [2], from these techniques, sol-gel deposition is preferred in the preparation of high-quality ZnO thin films due to its low cost, simplicity and ability to deposit large area films [3]. The quality, structure and properties of ZnO thin films are influenced by fabrication parameters and techniques used [4]. Defects in semiconductors may be impurities or crystalline defects. Impurities can be introduced either intentionally or unintentionally during crystal growth and device processing [5]. The performance of ZnO-based devices is affected by the presence of impurity atoms and point defects such as oxygen vacancies and Zn interstitials because these defects create electronic states in the band gap of ZnO [6,7].

For space applications, the devices should be operating in harsh radiation conditions and information of radiation effects on devices performance is required. The effect of alpha particle and high energy electron irradiation on ZnO has been reported [8,9]. To the best our knowledge, there is no research available regarding the exposure of sol-gel ZnO thin films to alpha particle irradiation studied using DLTS and LDLTS techniques. In this work, the effect of alpha particle irradiation on the electrical properties of sol-gel ZnO thin films was studied using *I-V*, *C-V*, DLTS and L-DLTS techniques.

2. Experimental

ZnO solution was prepared by dissolving zinc acetate dihydrate in isopropanol. Monoethanolamine (MEA) was added to the solution, maintaining a molar ratio of MEA to zinc acetate dihydrate of 1.0 and the concentration of zinc acetate of 0.5 M. The solution was continuously stirred for 2 h at 60 °C to obtain a homogeneous and clear solution. This solution was aged for 48 h.

The ZnO solution was deposited on ITO/glass and n-Si substrates by sol-gel spin coating. Before deposition ITO/glass was cleaned in a three-step procedure, using acetone, ethanol and deionized water in an ultrasonic bath and dried in flowing N_2. A n-Si substrate (13–17 μm thick with a resistivity of 1.4–1.8 Ωcm) was cleaned using trichloroethylene followed by isopropanol, then methanol and rinsed in deionized water, each step was carried out for 5 min in an ultrasonic bath. Thereafter, the n-Si substrate was etched using hydrofluoric acid to remove the native oxide and dried in flowing N_2. The substrates (ITO/glass and n-Si) were spin coated at 4000 rpm for 40 s whilst the aged solution dropped onto

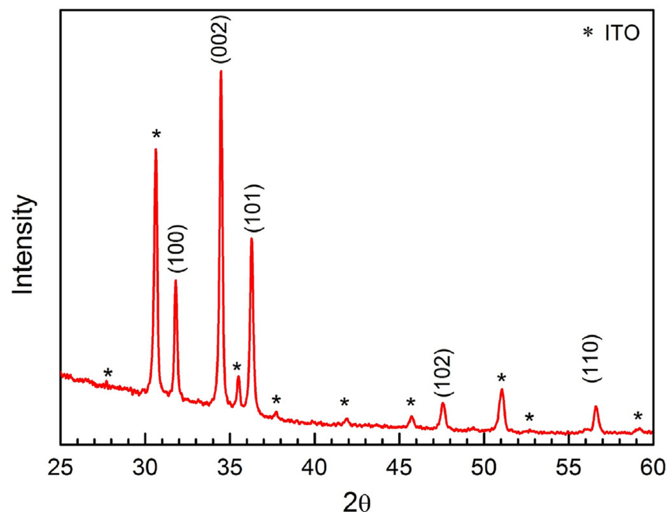

Fig. 1. The X-ray diffraction (XRD) patterns of ZnO thin films deposited onto ITO/glass substrate after annealing at 600 °C.

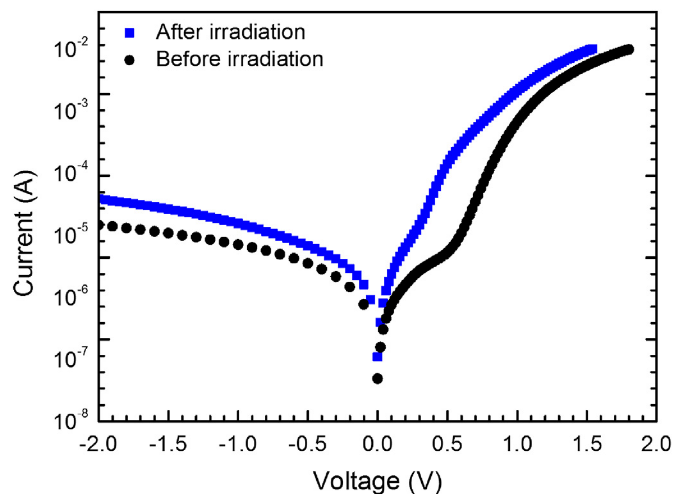

Fig. 2. Room temperature semi-logarithmic plot of *I-V* measurements of Pd/ZnO/n-Si/AuSb Schottky diode before and after irradiation with alpha-particles.

the substrates. The film was then dried at 200 °C. The coating and drying steps were repeated several times to obtain the desired thickness. The final films were annealed at 600 °C in air for 1 h.

The ITO/glass substrate was used for structure, surface and optical characterizations, whilst n-Si substrate was used for electrical and defects characterizations.

To form an ohmic contact on the back side of the n-Si, 150 nm thick AuSb (94 : 6) was resistively deposited and then annealed at 350 °C in Ar to improve the series resistance of the contact. Finally, Pd contacts, 0.60 mm in diameter and 100 nm thickness, were resistively deposited on the ZnO layer.

The sample was irradiated at room temperature with 5.4 MeV alpha particles from an Am-241 radionuclide for 21 h at a flux of $7.1 \times 10^6\ cm^{-2}s^{-1}$, through the Schottky contact.

3. Results and discussion

Fig. 1 shows the X-ray diffraction (XPERT-PRO diffractometer, PAN analytical BV, Netherlands) patterns of ZnO thin films deposited onto ITO/glass substrate. In the XRD patterns, there are strong peaks corresponding to the (100), (002) and (101) planes. Small peaks corresponding to the (102) and (110) planes were also observed, indicating that the films have hexagonal wurtzite structure. It is clear from this pattern that the films consist of randomly orientated polycrystalline particles with a slightly preferred orientation along (002) plane. The values of the lattice constants obtained are in good agreement with the values from the JCPDS data with card number (76-0704) and are shown in Table 1. The crystallite size *D* of the ZnO thin films was calculated from Scherrer's equation [10].

The surface morphology and cross-section of the films were studied using scanning electron microscopy (SEM). The thickness of the films was found to be ~ 800 nm as reported previously [11].

Fig. 2 shows the room temperature *I-V* characteristics of fabricated Pd/ZnO/n-Si/AuSb Schottky barrier diodes before and after alpha particle irradiation. The rectification before and after irradiation were 3 and 2.5 orders of magnitude, respectively.

Before alpha particle irradiation the diode exhibited generation-recombination effects at voltages lower than 0.5 V causing the kink in the forward bias curve, above this voltage thermionic emission is the dominant current transport mechanism across the Schottky barrier. At voltages V > 1.0 V, the diode characteristics deviated from linearity due to series resistance. After irradiation generation-recombination is observed at voltages lower than 0.2 V. Above that, thermionic emission was dominant and the diode deviated from linearity at high voltage due to the series resistance.

The diode parameters shown in Table 2 were calculated by performing a linear fit in forward bias region using thermionic emission theory [12].

Irradiation caused an increase in leakage current and ideality factor as well as a decrease in series resistance and the Schottky barrier height (SBH). The increase in leakage current and ideality factor are attributed to irradiation induced defects and interface states in ZnO thin films [6].

The *C-V* characteristics before and after irradiation at room temperature are shown in Fig. 3 (a). Fig. 3 (b) shows the $1/C^2$ vs V curves which are split into two regions reverse bias and forward bias. The free carrier concentration calculated from the reverse bias curve of ~ $10^{15}\ cm^{-3}$, and is related to n-Si. On the other hand, the free carrier concentration calculated from the forward bias curve (see Fig. 3 (b) inset) of ~ $10^{17}\ cm^{-3}$, indicating that this free carrier concentration is related to ZnO. The capacitance and free carrier concentration (N_D) decreased after irradiation. E. Gür et al. [13] observe the decrease of the capacitance and free carrier concentration after studying the effects of high energy electron irradiation on electrical properties of Au/n-ZnO Schottky diodes and attributed the decrease in the carrier concentration to the trapping effect of the deep defect states produced by high energy electron irradiation. The Schottky barrier height obtained from *C-V* measurements is greater than that obtained from *I-V* measurements, this due to inhomogeneity in SBH and image force effects [14].

Fig. 4 shows the energy band diagram of the Pd/ZnO/n-Si heterojunction at equilibrium and after applying the bias, constructed based

Table 1
Structural and lattice parameters of ZnO thin films.

FWHM	2θ		D (nm)	2δ (nm)	Lattice constants (Å)		Lattice constants (Å) from (JCPDS)	
(002)	(100)	(002)	(002)	(002)	a (100)	c (002)	a	c
0.181	31.805	34.477	48	0.0004	3.246	5.198	3.253	5.213

Table 2
The Schottky diode parameters from *I-V* measurements before and after irradiation.

Events	*SBH* (eV)		Ideality	Saturation current, I_s	Series	N_D (cm^{-3}) (C-V)
	I-V	*C-V*	Factor *(n)*	(A)$\times 10^{-9}$	Resistance (Ω)	$\times 10^{17}$
Before irradiation	0.635	1.24	3.41	11.2	53	12
After irradiation	0.536	1.18	3.48	519	43	4.0

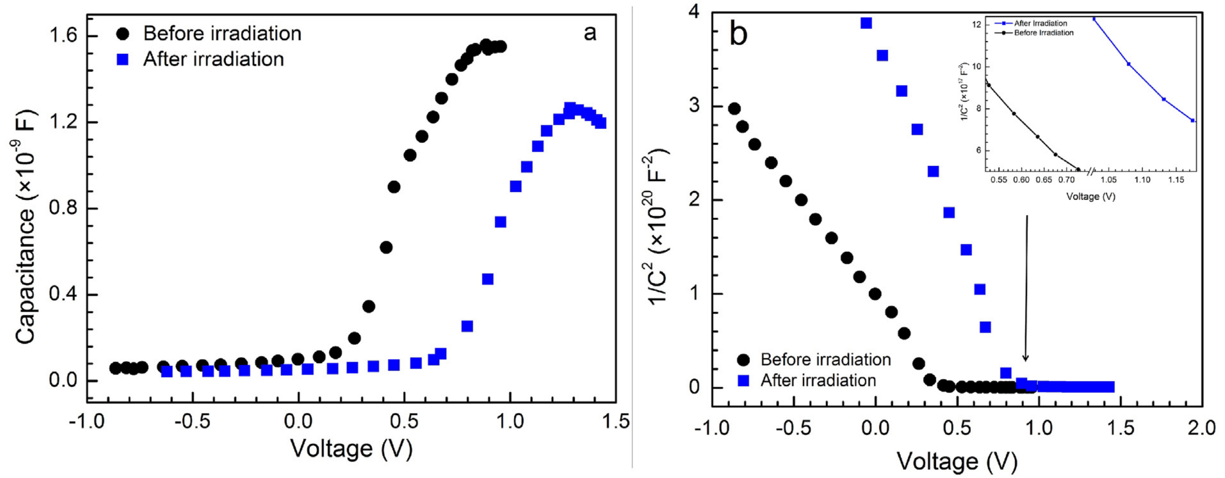

Fig. 3. *C-V* measurements before and after irradiation at room temperature at 1 MHz.

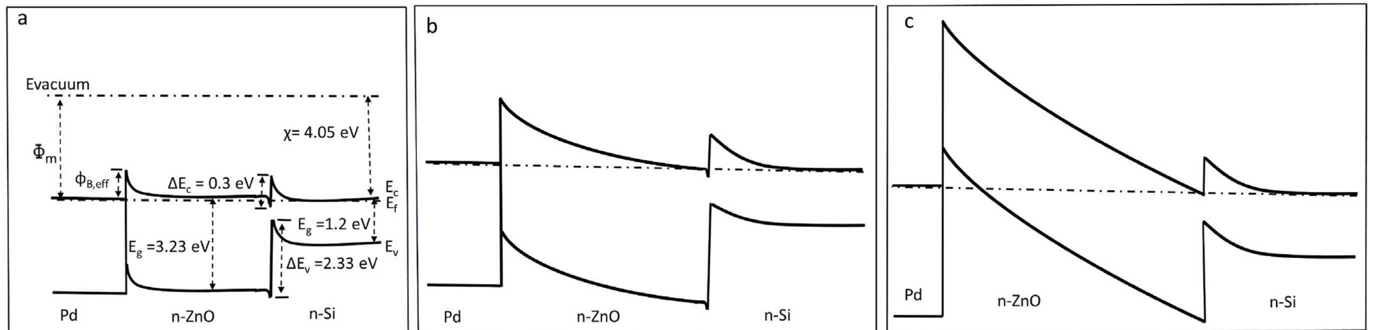

Fig. 4. Energy band diagram of Pd/ZnO/n-Si heterojunction (a) Under thermal equilibrium (b) After applying a small reverse bias (c) After increasing the reverse bias.

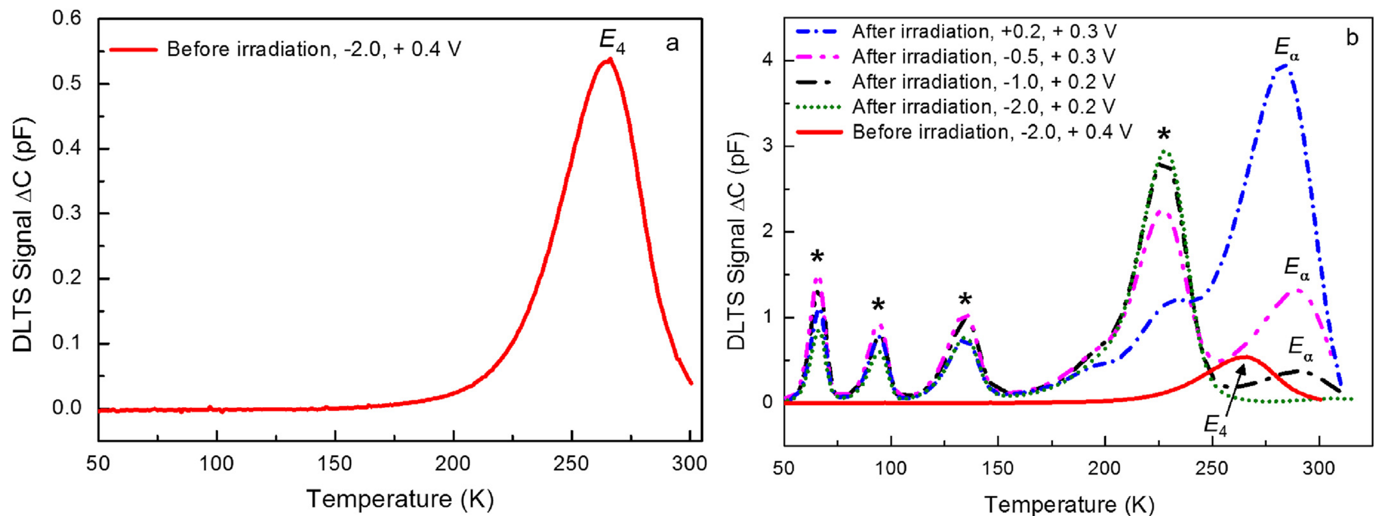

Fig. 5. DLTS spectra obtained from Pd/ZnO/n-Si/AuSb Schottky diode (a) before and (b) after irradiation, recorded at different a quiescent reverse bias, different amplitude of the filling pulse, filling pulse width of 1 ms and rate window of 80.2 Hz in the temperature range 20–350 K.

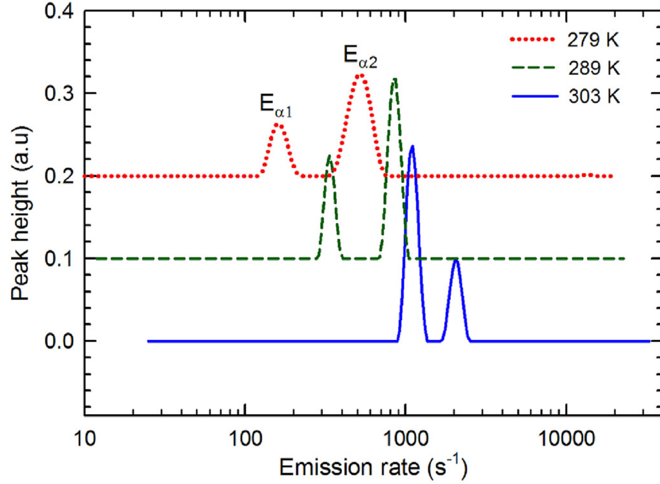

Fig. 6. Laplace DLTS spectra showing the shift of $E_{\alpha 1}$ and $E_{\alpha 2}$ defects at three temperatures in ZnO thin films after irradiation.

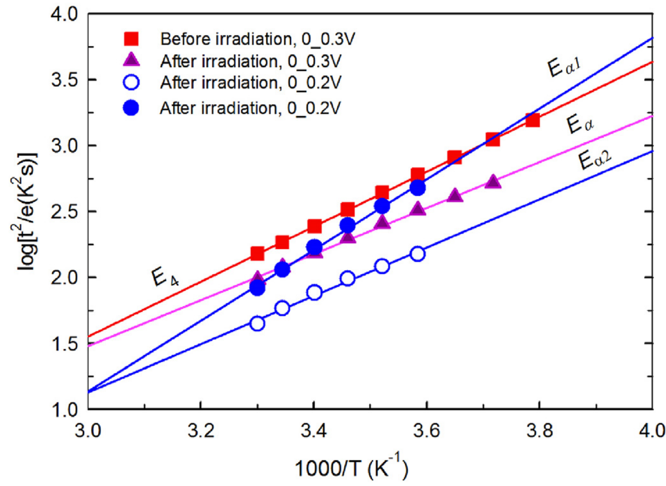

Fig. 7. Arrhenius plots of the defects in ZnO thin films, obtained at a quiescent reverse bias of 0 V with a filling pulse amplitude of 0.3 V for E_4, E_α and 0.2 V for $E_{\alpha 1}$ and $E_{\alpha 2}$. The filling pulse width was 1 ms.

Table 3
The defect energy E_T below conduction band and the apparent capture cross-section σ_{ap} of defects in ZnO thin films deposited on the n-Si substrate.

Defect label	$E_T(eV)$	$\sigma_{ap}(cm^2)$
E_4	0.41	4.8×10^{-16}
E_α	0.35	5.7×10^{-17}
$E_{\alpha 1}$	0.53	7.7×10^{-14}
$E_{\alpha 2}$	0.36	2.3×10^{-16}

on Anderson's model [15]. Both the ZnO thin film and the Si are n-type semiconductors with carrier concentration N_D of $12 \times 10^{17}\text{cm}^{-3}$ and $\sim 10^{15}\ \text{cm}^{-3}$, respectively calculated from *C-V* measurements. Thus, the Fermi level in n-ZnO and n-Si should as close to the conduction band edge at equilibrium (see Fig. 4 (a)). For n-type semiconductors the Schottky barrier height is predicted by Ref. [16]:

$$\phi_{B,eff} = \Phi_m - \chi_s \tag{1}$$

where Φ_m is the work function of Pd metal = 5.12 eV and χ_s is the electron affinity of ZnO = 4.35 eV [17]. Thus, The $\phi_{B,eff}$ calculated of 0.77 eV. The SBH calculated before and after irradiation of 0.635 eV and 0.536 from *I-V* measurements and 1.24 eV and 1.18 eV from *C-V* measurements. The $\phi_{B,eff}$ obtained from simple theory is greater than $\phi_{B,eff}$ obtained from *I-V* measurements and smaller than $\phi_{B,eff}$ from *C-V* measurements. The difference in simple theory and experimental results of SBH is due to the presence of surface states and SBH inhomogeneity at the Pd/ZnO interface.

According to Anderson's model, the conduction band offset and valence band offset is given by:

$$\Delta E_C = \chi_{ZnO} - \chi_{Si} \tag{2}$$

$$\Delta E_v = (E_{gZnO} - E_{gSi}) + \Delta E_C \tag{3}$$

where χ_{Si} electron affinity of Si = 4.05 eV [18], thus ΔE_C calculated of 0.3 eV.

From equation (3) E_{gZnO} is the band gap of ZnO of 3.23 eV calculated from Tauc's plot (not shown here), E_{gSi} is the band gap of n-Si of 1.20 eV, so the valance band offset ΔE_v calculated of 2.33 eV. The smaller value of conduction band offset than valence band offset suggests that concentration of the electrons injected from n-ZnO into n-Si is greater than that of holes injected from n-Si into n-ZnO.

The DLTS spectrum exhibited one peak before irradiation labelled E_4, Fig. 5 (a). This defect has been observed by Auret et al. [19] in vapour-phase-grown single-crystal ZnO. Mtangi et al. [20] also observed this peak in bulk ZnO and they attributed it to the oxygen vacancy.

Fig. 5 (b) shows the presence of a new peak labelled E_α, introduced by α-irradiation. Using Laplace DLTS under reduced bias (see Fig. 6), the E_α was found to be made up of two energy levels $E_{\alpha 1}$ and $E_{\alpha 2}$ at 0.53 eV and 0.36 eV respectively, below the conduction band. The shift in Laplace DLTS spectra of $E_{\alpha 1}$ and $E_{\alpha 2}$ defects measured at three temperatures are displayed in Fig. 6. The apparent capture cross sections of $E_{\alpha 1}$ and $E_{\alpha 2}$ were calculated from Arrhenius plots, Fig. 7, and found to be $7.7 \times 10^{-14}\ \text{cm}^2$ and $2.3 \times 10^{-16}\ \text{cm}^2$, respectively. The uniqueness in activation enthalpy and apparent cross sections means that these defects are different. The electronic properties are summarized in Table 3.

There are four peaks observed in all curves (see Fig. 5 (b)) after irradiation located below 250 K and labelled by (*), their signatures are attributed to defects in the n-Si substrate. Under a quiescent reverse bias of −2.0 V and filling pulse amplitude V_p = 2.2 V, only defects in the n-Si were observed, as shown by the dotted curve (green) in Fig. 5 (b).

4. Conclusion

The structure of ZnO thin films deposited by the sol-gel technique showed the films to have hexagonal wurtzite structure, with a crystallite size of 48 nm.

From *I-V* and *C-V* characteristics, the SBH decreased after alpha particle irradiation and ideality factor and leakage current increased. The DLTS technique was used to identify the defects in the ZnO thin films before and after irradiation. It revealed defects before irradiation with an activation enthalpy of 0.41 eV. The defect with energy level 0.35 eV below the conduction band was observed after alpha particle irradiation. The 0.35 eV level was split using L-DLTS and found to consist of two defects at 0.53 eV and 0.36 eV. The relative heights of the peaks changed with biasing conditions, showing that the depletion region could be manipulated to profile through the ZnO-Si heterojunction.

Acknowledgments

This work is based on the research supported by the National Research Foundation of South Africa (NRF), under grant number 111744. The opinions, findings and conclusions or recommendations are that of the authors, and the NRF accepts no liability, whatsoever, in this regard.

References

[1] C. Mao, W. Li, F. Wu, Y. Dou, L. Fang, H. Ruan, C. Kong, J. Mater. Sci. Mater. Electron. 26 (2015) 8732.
[2] M. Saleem, L. Fang, A. Wakeel, M. Rashad, C. Kong, World J. Condens. Matter Phys. 2 (2012) 10.
[3] G. Murugadoss, R. Jayavel, M.R. Kumar, Superlattice. Microst. 82 (2015) 538.
[4] X. Meng, B. Lin, B. Gu, J. Zhu, Z. Fu, Solid State Commun. 135 (2005) 411.
[5] D.K. Schroder, Semiconductor Material and Device Characterization, 3rd ed., John Wiley & Sons, 2006.
[6] M.A. Salari, B. Güzeldir, M. Sağlam, AIP Conference Proceedings, vol. 1935, AIP Publishing, 2018, p. 050002.
[7] I. Procházka, J. Cizek, F. Lukac, O. Melikhova, J. Valenta, V. Havránek, W. Anwand, V.A. Skuratov, T.S. Strukova, Journal of Physics: Conference Series, vol. 674, 2016, p. 012014.
[8] J. Nel, F. Auret, L. Wu, M. Legodi, W. Meyer, M. Hayes, Sensors, B. Actuators, Chemicals 100 (2004) 270.
[9] C. Coskun, N. Gedik, E. Balcı, Semicond. Sci. Technol. 21 (2006) 1656.
[10] B. Cullity, S. Stock, Elements of X-Ray Diffraction, 3rd ed., Prentice-Hall, 2001.[11] J.M. Nel, M.E.I. Ahmed, M.A.M. Ahmed, W.E. Meyer, Proc.SPIE 11043, (2019), p. 11043.
[12] E. Rhoderick, R. Williams, Metal-semiconductor Contacts, 2nd ed., Clarendon Press, 1988.
[13] E. Gür, C. Coşkun, S. Tüzemen, J. Phys. D Appl. Phys. 41 (2008) 105301.
[14] S.S. Cohen, G.S. Gildenblat, Metal–Semiconductor Contacts and Devices vol. 13, Academic Press, 2014.
[15] R.L. Anderson, 5 Springer, 1962, p. 341.
[16] R. Enderlein, N.J. Horing, Fundamentals of Semiconductor Physics and Devices, World Scientific, 1997.
[17] F. Bedia, A. Bedia, B. Benyoucef, S. Hamzaoui, Physics Procedia 55 (2014) 61.
[18] M. Wei, C.-F. Li, X.-R. Deng, H. Deng, Energy Procedia 16 (2012) 76.
[19] F.D. Auret, S.A. Goodman, M.J. Legodi, W.E. Meyer, D.C. Look, Appl. Phys. Lett. 80 (2002) 1340.
[20] W. Mtangi, F.D. Auret, P.J. Janse van Rensburg, S.M. Coelho, M.J. Legodi, J. Nel, W. Meyer, A. Chawanda, J. Appl. Phys. 110 (2011) 094504.